# CFD calculations and PIV measurements on tank-in-tank heat store

**Eshagh Yazdanshenas[1], Simon Furbo[2], and Jianhua Fan[2]**

[1] Austrian Institute of Technology, Energy Department, Giefinggasse 2, 1210 Vienna, Austria

Phone: +43(0) 50550-6317, Fax: +43(0) 50550-6679, E-mail: Eshagh.Yazdanshenas@ait.ac.at

[2] Department of Civil Engineering, Technical University of Denmark, Building 118, DK-2800, Kgs. Lyngby, Denmark

**Abstract**

Theoretical and experimental investigations of a tank-in-tank heat storage for a solar combisystem have been carried out. The investigated combistore is designed for PIV measurement studies. The theoretical investigations are carried out by means of the Computational Fluid Dynamics CFD code Fluent 6.1 [1]. The tank-in-tank heat storage is a tank where the domestic hot-water (DHW) tank is placed in the space heating storage tank. The space heating storage tank is heated by the solar heat by circulating water through the outer tank. Heat is transferred from the space heating storage tank to the DHW tank through the tank wall of the DHW tank. A model of the heat storage tank used for experimental studies has been built up in the CFD program. The fluid motion and the thermal conditions for the heat store have been investigated during different operation conditions. It has been analyzed how the thermal stratification in the space-heating storage and DHW tank during periods with hot water consumption is influenced by hot water draw-off.

## 1. Introduction

Due to the fewer sources of fossil fuels availability and pollution problems it is important to develop renewable energy systems. Solar energy might become a major component of future sustainable energy supply in the form of solar thermal heating, photovoltaics (PV) and concentrating solar power (CSP).

Solar thermal systems consist of solar domestic hot water (SDHW) systems, solar combisystems for heating of buildings and domestic hot water supply, solar heating plants for heating a whole town or a part of a town by means of a district heating system, solar cooling systems, solar heating systems for desalination and purification of water and air collectors for dehumidification of buildings.

A report on the worldwide installed solar collector capacity prepared within the Solar Heating and Cooling Programme (SHC) of the International Energy Agency (IEA), [2] presents a study of the solar heating market. The study includes 49 countries with 4 billion people, which is about 60% of the world's population. The installed capacity in these countries is estimated to represent 85–90% of the solar thermal market worldwide. The solar thermal collector capacity in operation worldwide equalled 146.8 GWth corresponding to 209.7 million square meters at the end of the year 2007. Of this, 120.5 GWth were accounted for by flat-plate and evacuated tube collectors and 25.1 GWth by unglazed plastic collectors. The air collector capacity installed was 1.2 GWth.

A heat storage is needed in a solar heating system due to the time differences between the heat production of solar collectors and the heat demand. The heat can be stored in the heat storage until it is needed.

It is also not often possible that the solar heat covers the domestic hot water consumption and space heating demand 100%. Therefore the heat storage is generally built in such a way that it contains an auxiliary energy supply system to meet the domestic hot water consumption and space heating demand.

Many different Solar Combisystem designs have been commercialized over the years. In the IEA-SHC Task 26 [3], twenty one solar combisystems have been described and analyzed.

Tank-in-tank heat stores have the advantage of having high peak power on the demand side, low heat loss due to its compact design, no lime problems and a reduced hot water volume compared to hot water tanks which makes it easy to avoid restrictions in the design due to legionella considerations. Theoretical and experimental investigations of a tank-in-tank heat storage for a solar combisystem have been carried out. The investigated combistore is designed for PIV measurement studies. The theoretical investigations are carried out by means of the Computational Fluid Dynamics CFD code Fluent 6.1 [1].

## 2. Investigated tank-in-tank store

In Fig. 1, a picture of the investigated tank-in-tank heat store is shown. Three different materials are used for the tank-in-tank heat store. The upper part of the DHW tank is made from plastic. The lower part with smaller diameter is made of steel. The outer wall of the tank is made of glass. The store is heated up from the top to the bottom in the outer tank and can be discharged from the inner tank (DHW tank).

Fig. 1: Picture of the tank-in-tank heat store. The inner tank is for domestic hot water, whereas the outer tank is for water for space heating.

Table 1 shows the volume of space heating, domestic water in the heat store and the total volume respectively.

Table 1: The volume of domestic water and water for space heating in the tank.

| | Volume [l] |
|---|---|
| Domestic water, upper level | 19.8 |
| Domestic water, lower level | 9.7 |
| Water for space heating | 94.8 |
| Total | 124.3 |

The tank-in-tank heat store dimensions are shown in Fig. 2 at a vertical and a horizontal section, respectively. All dimensions are the inside diameter. The outside glass thickness is 12 mm and the inside plastic thickness is 4 mm.

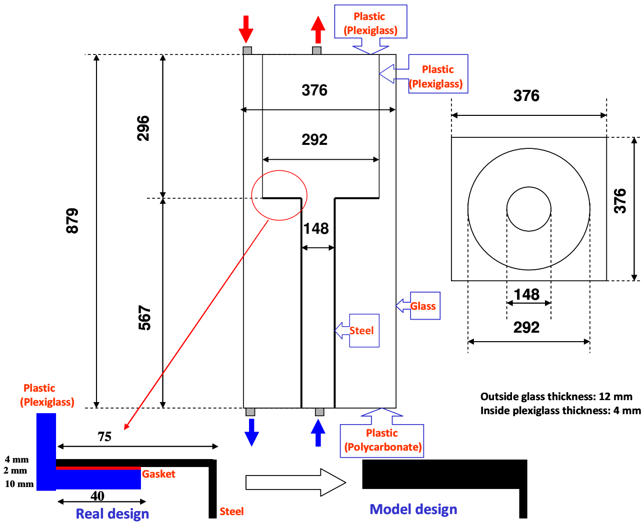


Fig. 2. Tank-in-tank heat storage dimensions. The dimensions are inside diameter.

## 3. CFD model of tank-in-tank

A model of the heat store has been built in Gambit. A number of simplifications have been made so that in FLUENT the final model of the heat store is somewhat simpler than the real heat store. The contact between the lower and upper wall material is in the CFD model simplified to a simpler geometry. Therefore, the thermal property of such a geometry is obtained and used for the simulations. Table 2 shows the thermal properties of the materials used in the model.
The model contains the water in the tank with the space heating section and the water in the inner domestic hot water tank. With the model it is possible to investigate how thermal stratification both in the inner and outer tank is established, and how the heat transfer into the domestic water will be during different operation conditions. Further, it is possible to investigate the natural convection in both tanks.

Table 2: Thermal properties of the used material in the model.

| Material | Density [kg/m³] | Cp [J/kg·K] | Thermal conductivity [W/m·K] |
|---|---|---|---|
| Glass | 840 | 2250 | 1 |
| Plastic (Polycarbonate) | 1200 | 1170 | 0.21 |
| Plastic (Plexiglass) | 950 | 1880 | 0.43 |
| Steel | 7830 | 434 | 64 |
| Steel-plastic combined | 2682 | 1070 | 0.67 |

In FLUENT the model of the heat store is divided into a computational mesh composed of small cells. One forth of the tanks is selected for the simulations because the geometry is symmetrical and it reduces the computational time. Fig. 3 shows the geometry of the model made in Gambit. The inlet and outlet to and from the DHW tank is located exactly at the middle of the DHW tank. The store volume is divided to many other volumes, so that the Cooper method that is used for meshing the geometry is applicable to the tank and also for defining the three different tank materials which are used for the tank. The inner and outer tanks as well as the tank materials are included in the model. First the middle volume is meshed, then the lower and finally the upper volume with the Hex-Cooper method with the interval size of 4 mm. Totally, 1167859 cells are used and checked in Gambit. The worst meshed element is found to have a skewness angle of 0.44. The skewness angle is a criteria that is between 0 to 1 and the lower this value is, the better the quality of mesh will be.

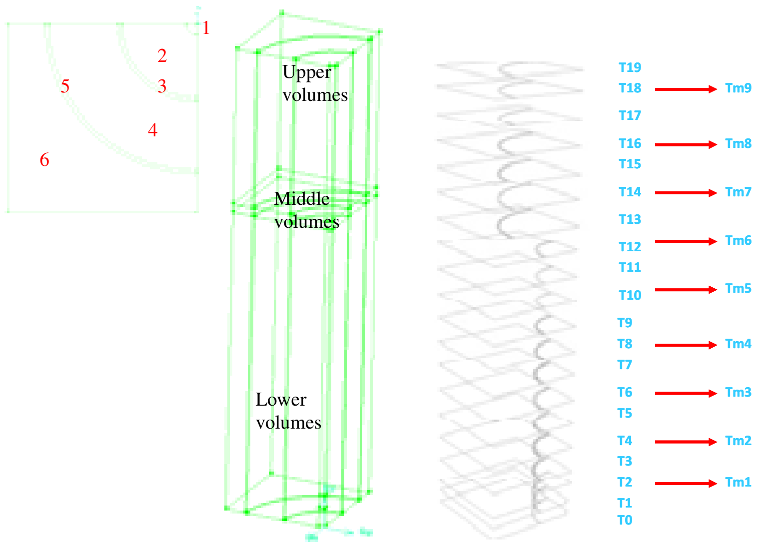


| | SH | DHW |
|---|---|---|
| T19 | 87.9 | 87.9 |
| T18 | 84.4 | 84.4 |
| T17 | 79.4 | 79.4 |
| T16 | 74.4 | 74.4 |
| T15 | 69.4 | 69.4 |
| T14 | 64.4 | 64.4 |
| T13 | 59.4 | 59.4 |
| T12 | 54.4 | 54.4 |
| T11 | 49.4 | 49.4 |
| T10 | 44.4 | 44.4 |
| T9 | 39.4 | 39.4 |
| T8 | 34.4 | 34.4 |
| T7 | 29.4 | 29.4 |
| T6 | 24.4 | 24.4 |
| T5 | 19.4 | 19.4 |
| T4 | 14.4 | 14.4 |
| T3 | 9.4 | 9.4 |
| T2 | 4.4 | 6.4 |
| T1 | 2.4 | 2.4 |
| T0 | 0 | 0 |

From the top Three dimensional geometry

Fig. 3: The tank geometry made in Gambit [left] and temperature sensor locations inside space heating and DHW tank in the CFD model and the measured tank [right].

Therefore the mesh quality is determined to be good enough for the CFD calculations in FLUENT. In FLUENT, for the boundary conditions, the ambient temperature is set to 20°C. The heat transfer coefficients through the upper, side and bottom walls are set to 3.56, 2.47 and 1.15 W/m²K for the tank with insulation. This corresponds to the measured tank heat loss. Water is a working fluid in the model and polynomial density is used for calculation of water density based on the following equation:

$$\rho(T)=863.559+1.21494.T-0.0025708.T^2 \quad (1)$$

where T is the variable temperature [K] and ρ is the density at the reference temperature [kg/m³].
The solver is pressure based and implicit method is used to solve the set of equations. Unsteady state condition is chosen so that it is possible to study the fluid flow and heat transfer in different time steps. Energy equation is also chosen to be solved together with Navier-Stokes equation. In the operating condition, the gravity is set to 9.806 m/s² and operating temperature is set to 35°C which is the mean temperature inside the tank.
It was found that a turbulent model is suitable for the natural convection inside the DHW tank and a laminar flow model is suitable in the outer tank (space heating tank) during DHW discharge. However, laminar model is used in both sides after DHW discharge and during standby. k-epsilon (k-ε) model for turbulence is used for modeling of turbulence in the tank. Turbulence, flow and energy equations are solved together with the SIMPLE algorithm for pressure-velocity coupling equations. Body forced weighted method which is suitable for buoyancy driven flow is used for interpolation scheme for discretization of the face pressure. First order upwind interpolation method is used for discretization of momentum, turbulent kinetic energy, turbulent dissipation rate and energy equations.
The property conservation is also checked. The mass flow rate imbalance is calculated as -2.79e-9 kg/s. A time step of 2 sec is used for the simulation and the maximum number of iterations per time step is 20 for the unsteady state condition. Number of time steps is chosen depending on the test period.

## 4. Comparison between experiments and CFD calculations

Simulations have been carried out with the built CFD-model of the tank-in-tank heat store. The aim of the simulations is to investigate the fluid motion and heat transfer in the tank during a number of typical operation conditions.

To begin with, during domestic hot water draw-off, the development of thermal stratification in the space heating storage tank and DHW tank and the development of the outlet temperature from the DHW tank are investigated.

Measured and calculated temperatures in 9 different levels in the heat storage are compared. The locations of the 9 levels are shown in Fig. 3.

In the investigations, the starting temperatures of 50ºC for both DHW and space heating tank are used, and the DHW tank is discharged with a volume flow rate of about 2.3, 4 and 6 l/min, and an inlet temperature to the DHW tank of about 20ºC. Of course, the flow rates and the inlet temperatures are set to the exact values of the measurements. The glass tank is with insulation. In one case the total DHW tank volume is discharged. The thermal stratification is investigated after the discharge.

### 4.1 Grid and time independency analysis

In any CFD modeling or numerical modeling, it is very important to establish grid and time independent results. Grid independence is achieved when further refinement or expansion of the grid does not result in significant changes to the converged CFD solutions. In unsteady state conditions, time independence is important. The governing equations in CFD are descretised and solved by a discrete grid of cells called mesh or grid. The number of grids should be as low as possible in order to save computational time while the mathematical error should be below a certain acceptable rate.

In this study three different mesh numbers of 0.8, 1.2 and 1.4 million have been investigated. Fig. 4 shows tank height versus the temperature distribution of DHW tank during discharge. The temperatures are averaged temperatures for the levels in question in the tank. The discharge flow rate is 2.3 l/min and the cold water inlet temperature is 20 ºC. The temperature distribution is for three different grid numbers. The simulation runs till the whole DHW tank volume is discharged corresponding to 12.83 min.

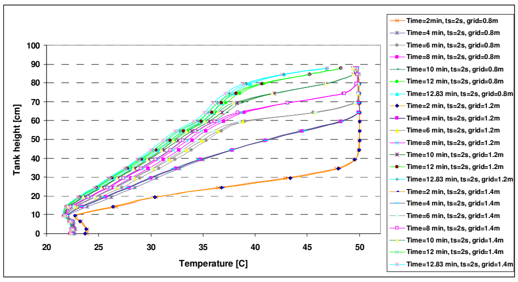

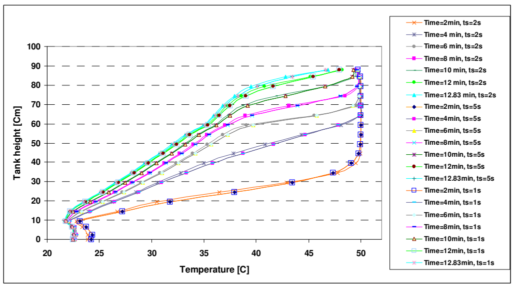


Fig. 4: Temperature distribution inside the DHW tank for different grid numbers [left] and for different time steps [right], discharge flow rate=2.3 l/min.

Based on Fig. 4, showing the temperature distribution in the inner and outer tank it is concluded that a grid number of 1.2 million is suitable for the CFD simulations while a grid number of 0.8 million is not capable of modeling the flow and heat transfer well and a grid number of 1.4 millions increases the computational time, without resulting in improved accuracy.

The time independency analysis was also carried out with three different time steps of 1, 2 and 5 seconds. The results of the time indecency are shown in Fig. 4.

The results with time steps of 1 and 2 second are close to each other, while a time step of 5 s is not suitable for the simulation since the temperature prediction is not the same as for 1 and 2 s. Therefore, a time step of 2 s is chosen as the best time step where a good accuracy and a short computational time will be achieved.

## 4.2 Comparison of thermal measurements and calculations

The test is carried out with an initial temperature of 50ºC, a DHW volume flow rate of 4 l/min and an inlet temperature of about 20ºC for the insulated tank. The whole DHW tank volume is discharged. Fig. 5 shows the temperature distribution inside the DHW tank. The temperature inside the tank is decreasing when the discharge is started and continues decreasing till 505 sec. After the discharge, the tank remains stand still without any discharge and the temperature inside DHW tank starts increasing due to heat transfer from the outer tank. Due to the time consumption of the CFD work, only 1 hour of the test has been calculated. The calculated temperatures are temperatures where the temperature sensors are placed. There is a good agreement between measured and calculated temperatures inside the DHW tank.

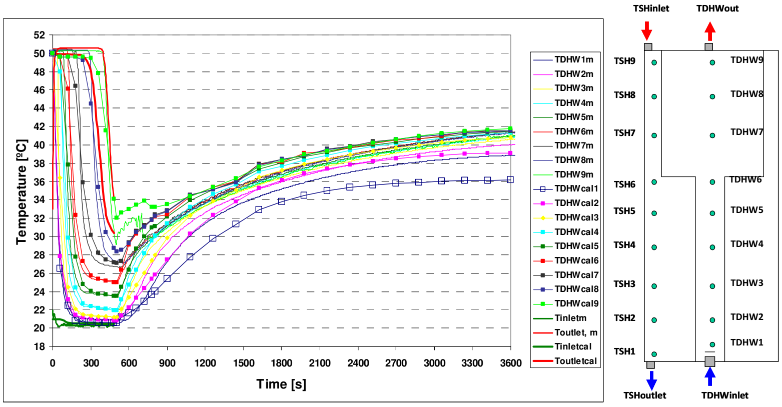


Fig. 5: Calculated and measured temperature distribution inside the DHW tank for discharge flow rate of 4 l/min.

The temperature distribution of the outer space heating store is shown in Fig. 6. The agreement between calculated and measured temperatures is better for the bottom of the tank than for the upper level of the tank. The temperature sensor TSH9 is located close to the inlet to the space heating tank. This temperature fluctuates due to the high heat loss of the pipe connection due to the thermal bridge. All in all, it is concluded that there is a reasonable agreement between measured and calculated temperatures.

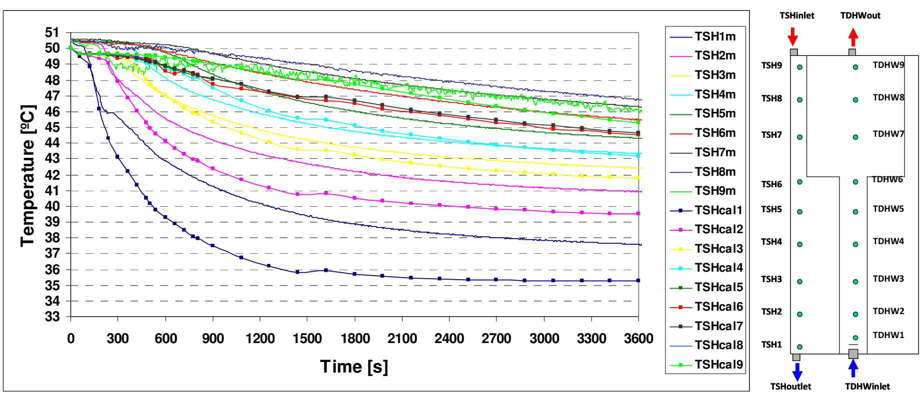


Fig. 6: Calculated and measured temperature distribution inside the space heating tank for discharge flow rate of 4 l/min.

## 4.3 Comparison of PIV measurements and CFD calculations

In order to validate the CFD model, the tank-in-tank system is experimentally investigated by means of PIV (Particle Image Velocimetry). In the inner tank, the fluid velocity was measured in the upper part of the DHW tank with a large tank diameter. The measurement area in the inner tank was divided into 2 sections and in the outer tank, it is divided to 4 sections as shown in Fig. 7.

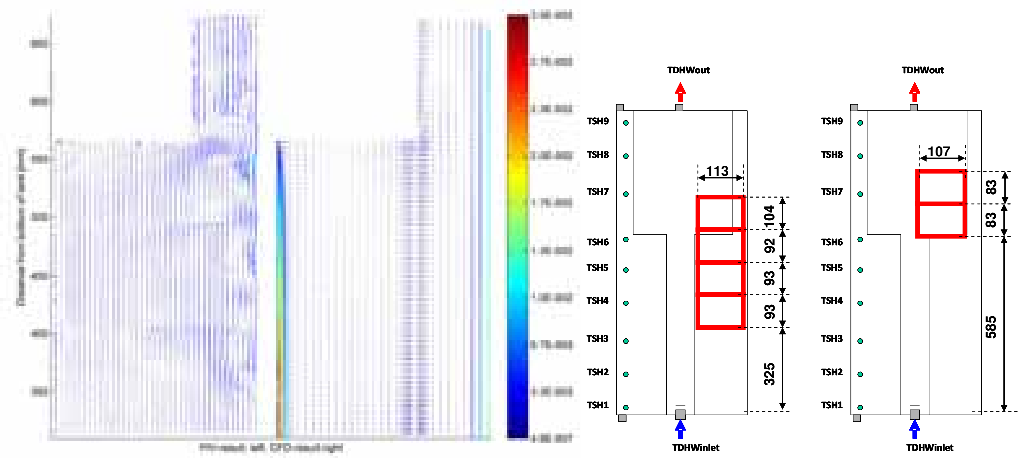


Fig. 7: Comparison of CFD and PIV flow field for the space heating tank during discharge after 2 minutes.

The uninsulated tank is first charged to 50ºC and after reaching stability, the discharge test is started with an inlet temperature of 20ºC and a volume flow rate of 4.5 l/min for about 6.5 minutes. CFD calculations and PIV results are compared during and after the discharge. Fig. 7 shows the measured flow field in the outer tank in 4 different sections which are glued together after 2 minutes of discharge. There is a downward flow close to the steel wall at lower levels of the tank. This downward flow can be visualized better in CFD than PIV. The downward flow close to the steel wall can not be seen well in the PIV measurements because the steel tank wall reflects the laser lights which cause that the camera could not take a good quality picture close to the steel tank wall.

There is a downward flow in the narrow upper level of the outer tank and it is higher close to the glass tank than the middle of the tank. This higher velocity close to the glass tank wall is due to a high heat loss. There is upward flow shown in both CFD and PIV at the middle of the narrow upper level of the tank. In the region where the diameter of the lower and upper tank is changed, the flow structure is slightly different from the rest of the tank. In this region, the upward flow coming from the lower part of the tank meets the downward flow caused by heat loss. Therefore some flows go upward at the middle of the narrow region and some flow back to the lower tank. Consequently at this region, a rotating region appears which is due to the sudden change in diameter and the upward and downward flow. This appears clearly from the PIV measurements. The result for the discharge after 2 minutes shows quite a good prediction by CFD simulations. The velocity range in the tank is from 0 to 30 mm/s.

The inner DHW tank flow field is also investigated by means of CFD and PIV as shown in Fig. 8. The main reason for choosing the region where the tank diameter is changing is to visualize how the fluid flow behavior is influenced by the change in diameter of the inner tank in the tank-in-tank heat store. Therefore the same experiments were carried out for the inner tank as well. Two sections are glued together as it is shown. The tank is first charged to 50ºC and after reaching stability, the discharge test is started with an inlet temperature of 20ºC and a volume flow rate of 4.5 l/min for about 6.5 minutes.

Fig. 8 shows the flow field of the inner tank 2 minutes after the discharge. There is an upward flow coming from the lower tank with smaller diameter to the upper tank with larger diameter. The upward flow when reaching the larger diameter turns to the right part of the tank and then it returns back from the corner of the tank to the center of the tank. The flow from the center of the tank then continues moving to the right and then center of the flow field again. And they finally reaches and points to the outlet located at the top of the investigated region.

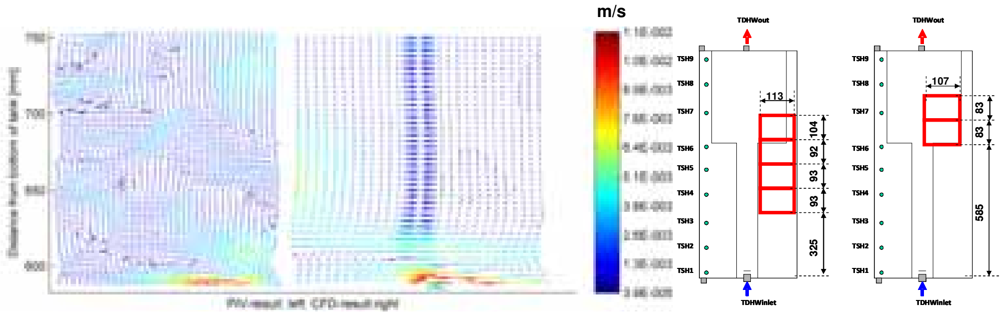


Fig. 8: Comparison of CFD and PIV flow field for the space heating tank during discharge after 2 minutes.

## 5. Conclusion

The purpose of this paper is to validate a CFD model of a tank-in-tank store during and after DHW discharge. The discharge DHW tests are carried out by means of PIV measurements and thermal experiments. The CFD calculations show that during DHW discharge, a turbulent model can be applied for modeling of the inner DHW tank and for the outer tank. A laminar model can be used when the DHW discharge is stopped both for the inner and the outer tank.
The comparison between the CFD and thermal experiments shows a good agreement between calculated and measured temperatures. And also there is a very good agreement between PIV measurements and CFD calculations on flow velocities.
Based on the theoretical and experimental investigations, it can be concluded that the CFD model has the capability to predict and simulate the heat transfer, flow velocities and temperature distribution in the tank-in-tank store in a reasonable way.

## Acknowledgements

This research study was supported by the European Union 6th research framework program, Marie-Curie early stage research training network Advanced solar heating and cooling for buildings - SOLNET.

## References

[1] Fluent 6.1 User's Guide, (2003). Fluent Inc. Centerra Resource Park 10 Cavendish Court Lebanon, NH 03766.

[2] W. Weiss, I. Bergmann, G. Faninger, (2009). Solar Heat Worldwide – Markets and Contribution to the Energy Supply 2007, IEA-SHC, http://www.iea-shc.org.

[3] W. Weiss, (2003). Solar heating systems for houses- A design handbook for solar combisystems, James and James, London, ISBN 1-902916-46-8.